*Proc. Natl. Acad. Sci. USA*
Vol. 86, pp. 1816–1820, March 1989
Biochemistry

# Crystal lattice packing is important in determining the bend of a DNA dodecamer containing an adenine tract

(x-ray crystallography/DNA structure)

ANNA D. DIGABRIELE, MARK R. SANDERSON*, AND THOMAS A. STEITZ

Departments of Chemistry, Molecular Biophysics and Biochemistry, and Howard Hughes Medical Institute, Yale University, 260 Whitney Avenue, New Haven, CT 06511

*Communicated by Donald M. Crothers, December 9, 1988*

**ABSTRACT** **The crystal structure of a DNA duplex dodecamer d(CGCAAAAATGCG) and its complementary strand has been determined at 2.6-Å resolution. Although our goal was to deduce the structural features of the static bending of the helical axis exhibited by adenine-tract structures in solution, we conclude that the overall bend of 20° in the direction of the major groove observed here arises from the forces associated with crystal packing. An isomorphous dodecamer brominated on one strand provides experimental evidence that this asymmetric sequence is positioned in two orientations in the crystal lattice that are related by a 180° rotation around the pseudodyad axis of the sequence. The bend in these two differently positioned DNA molecules depends on their orientation in the crystal, not on their sequence. As with previously determined structures containing adenine tracts, the adenine and thymine base pairs are highly propeller twisted. The N-6 of the adenine comes within hydrogen bonding distance of the O-4 of thymine one step down the helix, facilitating the formation of a series of bifurcated hydrogen bonds within the adenine tract. The adenine tract is relatively straight and the bending is localized outside this region.**

Sequence-dependent curvature of the helical axis of DNA is one of the most intriguing departures of DNA structure from the canonical B form of Watson and Crick. Intrinsic bending of a naturally occurring DNA in the absence of protein was first observed experimentally in a 490-base-pair restriction fragment of *Leishmania tarentolae* kinetoplast DNA, which was found to possess unusual physical properties, most notably anomalous migration in polyacrylamide gels (1). Subsequent experiments using differential decay of birefringence (2) and electron microscopy (3) have confirmed the presence of static curvature in kinetoplast DNA minicircles. The bending region possesses five or six adjacent adenine residues (A-tract), separated by cytosine- and guanine-rich sequences, and repeated at 10-base-pair intervals (4). More recently, DNA bending has been found in other naturally occurring A+T-rich regions of DNA that are essential for protein binding and regulation (5–9).

Several hypotheses for how A+T-rich sequences produce a static curvature in the helical axis of DNA have been advanced. The wedge model formulated by Trifonov (10, 11) proposes that adjacent base pairs are slightly nonparallel, thereby forming a wedge between them and bending the helical axis in a continuous fashion. Each base-pair wedge can be decomposed into roll and tilt components that are consistent with observed gel mobility data for certain A-tract sequences (12). By contrast, the junction model postulates that the bends occur at the junctions between the A tract, which has an alternate conformation, and the flanking DNA, which is in the B form (13). Recent calibration of DNA curvature has led to the prediction of specific values for roll and tilt angles at these 5′ and 3′ junctions (14).

Two crystal structures of deoxyoligomers possessing short A tracts were published while this work was in progress (15, 16). The structure of d(CGCAAAAAAGCG) and its complementary strand (15) was determined at 2.5 Å resolution and shows a bend of 20° in the direction of the major groove. The structures of d(CGCAAATTTGCG) (16) with and without distamycin bound to it have been determined to 2.2 and 2.5 Å, respectively. This DNA is bent 11° in the presence of distamycin and 15° in the absence of the drug.

In this study, the crystal structure of the dodecamer d(CGCAAAAATGCG) and its complementary strand d(CGCATTTTTGCG) has been determined at 2.6 Å to deduce the molecular requirements for sequence dependence of helical curvature. This dodecamer possesses a 20° bend of the helix axis toward the major groove, which is similar in magnitude and direction to the bend exhibited by d(CGCAAAAAAGCG) as well as to that observed in the "parent" structure of Dickerson and coworkers (17).

We conclude that neither the crystal structure reported here nor the previously reported structures (15, 16) provide structural information that directly shows the nature of the A-tract-induced bend that occurs in solution. Using a bromine derivative of d(CGCAAAAATGCG), we have obtained experimental evidence that this asymmetric DNA sequence is positioned in the crystal in two orientations related by a 180° rotation about its sequence pseudodyad axis. The coexistence of the two structures in the same lattice proves conclusively that the overall bend of this sequence, and presumably that of other DNAs that crystallize in the same lattice (15–17), must be due to crystal packing forces. Although the sequence is different in each orientation (Fig. 1), the bend is of the same magnitude and in the same direction for both helices; therefore, the overall bend cannot be sequence dependent.

## EXPERIMENTAL

DNA oligomers d(CGCAAAAATGCG), d(CGCATTTTTGCG), and the brominated sequence d[CGCA(BrU)TTTTGCG] were synthesized in 10-μmol amounts with an Applied Biosystems model 380A synthesizer. These sequences were chosen because five adenine residues flanked by a 5′ cytosine and a 3′ thymine exhibit the largest bend in gel-migration studies (13). Single-stranded oligonucleotides with the 5′-dimethoxytrityl group still attached were purified by reverse-phase high-performance liquid chromatography (HPLC). The dimethoxytrityl group was then removed by using glacial acetic acid, and the DNA was repurified by HPLC.

The publication costs of this article were defrayed in part by page charge payment. This article must therefore be hereby marked "*advertisement*" in accordance with 18 U.S.C. §1734 solely to indicate this fact.

*Present address: CRC Biomolecular Structure Unit, The Institute of Cancer Research, Sutton, Surrey, England.

Each strand was then desalted using a Sephadex G-15 gel filtration column equilibrated in 1 mM Tris·HCl/0.1 mM EDTA, pH 8.0 (1:10 TE buffer). Duplexes were formed by mixing complementary strands in appropriate amounts and were annealed by heating to 95°C and cooling slowly over a 2-hr period.

Crystals were grown from hanging drops (19) at 10°C from a solution of DNA (5 mg/ml) with 44 mM $MgCl_2$/10 mM sodium cacodylate, pH 7.0/40% (vol/vol) 2-methyl-2,4-pentanediol (MPD) as the crystallizing agent. They were stabilized at 4°C in a solution of 46 mM $MgCl_2$/10 mM sodium cacodylate, pH 7.0/41% MPD. Crystals used for data collection were approximately 0.1 × 0.1 × 1 mm. The dodecamer crystallizes in the space group $P2_12_12_1$ with cell dimensions $a$ = 24.54 Å, $b$ = 40.32 Å, and $c$ = 65.86 Å.

Each data set was obtained from a single crystal at 12°C using a Xuong-Hamlin Mark II area detector (20). The data were corrected for background, Lorentz, and polarization and were scaled using the Nielsen–Anderson area detector software (21). The $R$ factors on intensity between Friedel pairs were 4.9% for the native DNA and 7.0% for the brominated DNA. Further crystallographic calculations were done using the computer program PROTEIN (22).

Because these crystals are nearly isomorphous with those of the dodecamer d(CGCGAATTCGCG) crystallized by Wing *et al.* (17), the phases derived from this structure (23) were used to phase a difference Fourier map using as coefficients $F$(native DNA) − $F$(brominated DNA). This difference electron density map showed two peaks (4 $\sigma$) per duplex, one arising from a bromine in a duplex oriented as the Dickerson dodecamer (17) ("up" helix) and the other arising from a bromine in a duplex corresponding to a rotation of 180° about the pseudodyad of the double helix ("down" helix). (See Fig. 1 for orientations and numbering conventions used and Fig. 2 for the map.)

The positional and occupancy parameters of these two bromine sites were refined against data from centrosymmetric projections and then against all data using the heavy-atom refinement program within PROTEIN (22). The occupancies of the two bromine sites are 56.5% for the site in the same sense as the Dickerson dodecamer (up) and 43.5% for the anti-sense (down).

The starting structures were obtained by fitting models to an electron-density map calculated by using experimental amplitudes and calculated phases. Because the experimental amplitudes from the Dickerson dodecamer are deposited in the Brookhaven Data Bank, a map with 2$F$(A tract) − $F$(Dickerson) as coefficients was calculated [where $F$(A tract) and $F$(Dickerson) are the observed structure factor amplitudes from the A-tract-containing and Dickerson dodecamers, respectively]. The resulting map was better fit by the refined A-tract structure than by the refined Dickerson structure (Fig. 3).

```
     1  2  3  4  5  6  7  8  9 10 11 12
5'   C  G  C  A  A  A  A  A  T  G  C  G  3'
     |  |  |  |  |  |  |  |  |  |  |  |
3'   G  C  G  T  T  T  T  T  A  C  G  C  5'
    24 23 22 21 20 19 18 17 16 15 14 13

    25 26 27 28 29 30 31 32 33 34 35 36
     C  G  C  A  T  T  T  T  T  G  C  G
     |  |  |  |  |  |  |  |  |  |  |  |
     G  C  G  T  A  A  A  A  A  C  G  C
    48 47 46 45 44 43 42 41 40 39 38 37
```

FIG. 1. DNA sequences and numbering convention for the two helix orientations in this crystal. The up helix is numbered 1–24, and the down helix, which is related to the former by a 180° rotation about the pseudodyad axis of the sequence, is numbered 25–48. Evidence for the existence of both helices in the crystal comes from the two peaks in a $F$(bromine) − $F$(native) difference electron-density map.

FIG. 2. Superimposed on the structure of d(CGCAAAAATGCG) is a difference electron-density map between crystals of a derivative sequence with a bromouridine at position 21 and the native crystals. Phases used were calculated from the coordinates of the Dickerson DNA dodecamer. Two peaks that arise from bromine substitution are the only 4 $\sigma$ (darker contours) peaks on the map. The other contour level pictured here is 2.5 $\sigma$. One bromine peak appears at position 21 (upper left), while the other appears at position 9 (lower right), which is where a bromine peak would appear if the helix brominated at position 21 were rotated 180° about the sequence pseudodyad axis.

Least-squares refinement on each individual helix was carried out using the NUCLSQ (24, 25) based on Hendrickson–Konnert PROLSQ (24). At the beginning of this refinement, the $R$ factors of the up helix and the down helix were 35.0% and 36.1%, respectively, for 2267 unique reflections with >0.5 $\sigma$ intensity from 10 to 2.5 Å resolution. After 24 cycles each of positional refinement in the resolution range 6–2.5 Å, the $R$ factors of the up helix and the down helix dropped to 25.6% and 26.5%, respectively. Throughout the course of refinement, the $R$ factor of the up helix was consistently 1–2% lower than that of the down helix. Six additional cycles each of individual isotropic B-factor refinement improved the $R$ factors still further to final values of 22.1% and 23.2% for the up and down helices, respectively, at the end of NUCLSQ refinement. No attempt was made to add water molecules at this point. Clearly, such small differences in refinement statistics would not be sufficient alone to distinguish among the three possibilities of (*i*) all helix up, (*ii*) all helix down, or (*iii*) various mixtures of both helix up and down.

To refine both helices together at their respective occupancies, the constrained-restrained least-squares refinement (CORELS) program (version 1.12) (27) was used. To reduce the parameter/data ratio, the dodecamers were partitioned into 24 sugar-base-base-sugar rigid groups, with the sugars in the C2′-*endo* conformation. All dihedral angles except those in the sugar ring were slowly released as refinement progressed. Cycles of positional refinement were alternated with cycles of group isotropic temperature factor and overall scale factor refinement. The initial $R$ factor for 2223 unique reflections with >0.5 $\sigma$ intensity between 8 and 2.5 Å was 26.2%. When the $R$ factor dropped to 21.5% but the geometry was not ideal, the DNA was refitted into a 2$F$(observed) − $F$(calculated) electron-density map using the interactive graphics of FRODO on an Evans and Sutherland PS300 graphics system. From this point, the geometry was slowly released, as positional and B-factor refinement continued. Throughout the course of CORELS refinement, difference Fourier maps were examined and 23 peaks with intensities >2 $\sigma$ were ultimately assigned to water molecules or magnesium ions based on their isotrop-

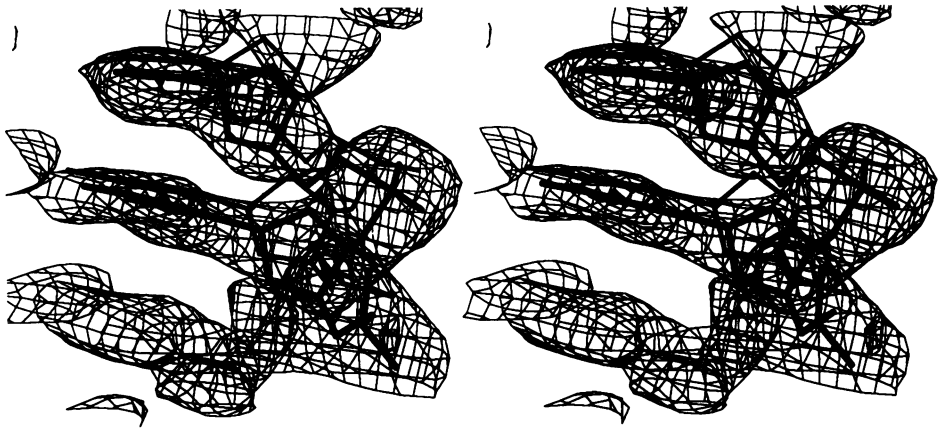

FIG. 3. Shown here is a portion of the initial electron density map computed using as coefficients $2F$(A tract) − $F$(Dickerson), where $F$(A tract) and $F$(Dickerson) are the observed structure factor amplitudes for the A-tract and Dickerson dodecamers, respectively, between 8 and 2.6 Å resolution, and phases derived from the Dickerson dodecamer (24); the final structure of d(CGCAAAAATGCG) (darker trace) and that from which the phases were derived (lighter trace) (18) are superimposed. The latter helix does not fit as well into this map, suggesting that this map, from which the initial model was derived, was not significantly biased by using the phases of the Dickerson dodecamer.

ic temperature factors. Refinement was stopped at an $R$ factor of 20.1% for 1975 reflections from 8 to 2.6 Å.

All helix parameters except for torsion angles were determined by using the Rosenberg–Dickerson helix analysis library. (For analytical expressions for quantities calculated, see the appendix of ref. 28 or see ref. 29.) Torsion angles for each helix were calculated by using the program CONFNUC, which is part of the NUCLSQ package (26).

Coordinates for both DNA helices as well as the observed structure factor amplitudes will be deposited in the Brookhaven Protein Data Base.

## RESULTS

A most important result arising from the structural determination of d(CGCAAAAATGCG) and its complement is the experimental evidence that an asymmetric DNA helix is positioned in the crystal in two orientations that are distinct because of the sequence asymmetry. A heavy atom derivative with one bromine atom per double helix was synthesized and crystallized isomorphously with the native dodecamer. However, the difference Fourier map (bromine−native) depicted in Fig. 2 exhibits two equally intense peaks attributed to bromine atoms, one at the position of the brominated base, position 21, and the other at position 9, which is where the brominated uridine base would be if the entire helix were rotated 180° about its pseudodyad axis (see Fig. 1). The relative occupancies of the two helix orientations were assumed to be those of the bromine atoms, and both helices were used as models refined against the observed structure factors.

Perhaps the most striking local structural feature of d(CGCAAAAATGCG) is the high degree of propeller twist exhibited by the adenine and thymine bases of the adenine tract (Table 1). The average propeller twist for this region is 20.3° for the up helix and 19.3° for the down helix, while the average propeller twist for the base pairs of the flanking regions is 9.9° for the up helix and 9.3° for the down helix. One consequence of this unusually large degree of propeller twist in the A tract is to bring into hydrogen-bonding proximity the adenine N-6 and the O-4 of the thymine of the adjacent base step, thus allowing the formation of bifurcated hydrogen bonds in the major groove of the DNA (32).

Nelson *et al.* (15) also noted that the helix axis of the A tract is straight. We see a similar trend for localization of the bend outside the adenine region. The up helix exhibits smaller roll and tilt angles within the A tract than outside it. The situation is not quite as clear in the case of the down helix upon examination of the roll and tilt parameters. Although they do exhibit smaller roll angles, the base steps in the adenine region of the down helix exhibit larger tilt angles than the base steps outside the A tract. The bends at the 5′ and 3′ junctions of the A tract are probably due mainly to roll.

The average helical twist of the DNA is 36.0° for the up helix and 36.6° for the down helix. The up helix possesses 9.9 residues per turn, while the down helix possesses 9.8 residues per turn. The average rise per residue for each helix is 3.3 Å. The conformation of all sugar residues was constrained to C2′-*endo*, and dihedral angles within the sugar ring were held fixed. For those torsion angles that were varied, we see no trends that can be attributed to a different structure in the A+T-rich region.

## DISCUSSION

We have experimentally established that an asymmetric DNA sequence can exist in a crystal in two orientations that are related by a 180° rotation about the sequence pseudodyad axis. These two orientations are distinct because of sequence asymmetry and must be treated as such during refinement. This evidence raises the possibility that crystals of other asymmetric DNA sequences may also contain the DNA in

Table 1. Comparison of propeller twist of four DNA structures

| Base pair | Up helix | Down helix | Nelson *et al.* helix (15) | Wing *et al.* helix (17) |
|---|---|---|---|---|
| 1 | 5.9 | 6.2 | 19.0 | 13.2 |
| 2 | 8.3 | 16.8 | 12.3 | 11.7 |
| 3 | 5.2 | 7.3 | 7.7 | 7.2 |
| 4 | 15.5 | 0.8 | 14.6 | 13.2 |
| 5 | 20.4 | 17.0 | 23.0 | 17.1 |
| 6 | 20.6 | 22.5 | 25.5 | 17.8 |
| 7 | 22.6 | 15.7 | 22.5 | 17.1 |
| 8 | 22.2 | 23.9 | 17.7 | 17.1 |
| 9 | 19.5 | 17.5 | 19.2 | 18.6 |
| 10 | 6.5 | 5.1 | 10.8 | 4.9 |
| 11 | 17.9 | 20.5 | 15.2 | 17.2 |
| 12 | 5.9 | 8.4 | 6.2 | 6.2 |

The parameters shown here for the up helix and the down helix were calculated by using the Rosenberg–Dickerson helix analysis library. The best helix axis for each helix using all base steps was calculated by the program AHELIX. The program BROLL was used to calculate propeller twist. Propeller twist is the dihedral angle between the normals of 2 bases in a base pair (30, 31). Base pair number 1 is $C^1 \cdot G^{24}$ for the up helix, as well as for the helices of Nelson *et al.* (15) and Wing *et al.* (17), and $C^{25} \cdot G^{48}$ for the down helix.

two orientations. However, the extent to which scrambling of the DNA orientation in the crystal is influenced by the degree of sequence asymmetry is incompletely established. DNA sequences that are more asymmetric than the one reported here may pack uniquely in crystals.

**Relevance of Bend in DNA Helix Axis.** The existence of the same DNA sequence in two different orientations in the crystal allows one to assess whether the observed bend in the DNA arises from the DNA sequence or its orientation and packing in the crystal. If the nucleotide sequence is the primary determinant of the bend, then the bend observed for the up and down helices should be the same when their sequences are identically aligned. If, however, crystal packing is dominant, then the two structures should be the same when oriented the same way in the crystal.

Because we observe here that the A-tract-containing DNA exhibits essentially the same bend when the up orientation is superimposed on the down orientation, we conclude that the overall bend is due to crystal packing forces and not to the A-tract sequence. Fig. 4 shows the bend in the helix axes for both the up and down helices as well as for the down helix rotated by 180° about its pseudodyad axis. This figure shows that the bends are in the opposite direction when the up and down helices are aligned with their sequences the same. Also, the bend in the Dickerson dodecamer can be seen to be closely similar to that of the up and down A-tract helices. The orientation of the DNA duplex in the crystal and not its sequence dictates the bend direction. From a detailed analysis of the effect of crystal packing on oligonucleotide double-helix structure, Dickerson *et al.* (33) conclude similarly that the requirements of efficient packing in a DNA crystal override the molecular symmetry of the oligomer. The completely symmetric sequence d(CGCGAATTCGCG) has an asymmetric bend in the crystal.

**Relevance of $dA_5 \cdot dT_5$ Structure.** It has recently been shown by Raman studies on A-tract DNA in solution and in crystals that the local structure of the DNA is preserved in both forms (34, 35), indicating that, although the overall bend in the helix axis is an artifact of crystal packing, the local structural features adopted by the DNA in a crystal may be consequences of the DNA sequence itself and not of the crystal lattice into which it is packed, as concluded earlier by Fratini *et al.* (28). Indeed, the local structures of A+T-rich regions of DNA crystal structures seem to demonstrate that these regions are different from the flanking DNA (15, 16, 28). The high degree of propeller twist exhibited by the adenine and thymine bases of the A tract (see Table 1) is a feature that is common to all of the oligo(dA)·oligo(dT)-containing structures determined thus far (15, 16). The unusually large propeller twist facilitates the formation of an additional hydrogen bond in the major groove of the DNA (32). This zigzag pattern of hydrogen bonds may serve to stiffen the DNA, making deformation within the A-tract region energetically less favorable (15). The lengths of the bifurcated hydrogen bonds (Table 2) are similar to those noted for the other A-tract structures (15, 16).

The values determined for helical twist and number of residues per turn for the structure reported here are in close agreement with those determined for the "parent" B-form dodecamer d(CGCGAATTCGCG) (28) and also for the A-tract sequence d(CGCAAAAAAGCG) (15) and are consistent with the 10.1-base-pair helical screw noted for poly(dA)·poly(dT) in other studies (30, 31).

Nelson *et al.* (15) suggested that the straight nature of the helix axis in the A-tract region is a natural consequence of the rigidity imparted by extra hydrogen bonds. They observed the presence of smaller tilt and roll angles for the base steps in the A tract than for the base steps outside this region, indicating that bending of the helix axis must be localized outside the A·T region in their crystal structure. They propose that the A-tract-induced bend in solution arises either from a large base-pair roll concentrated at the junctions between the A tract and the intervening sequences or is more widely distributed over the flanking regions that are themselves intrinsically bent. The former possibility would yield a bend direction that is inconsistent with solution experiments (13, 14, 36, 37), while the latter possibility might be more consistent.

The direction of the A-tract-induced bend deduced from various solution experiments by Crothers and coworkers (13, 14, 36, 37) is 90° from the bend direction observed in this crystal. If, as suggested by the solution experiments (13, 14,

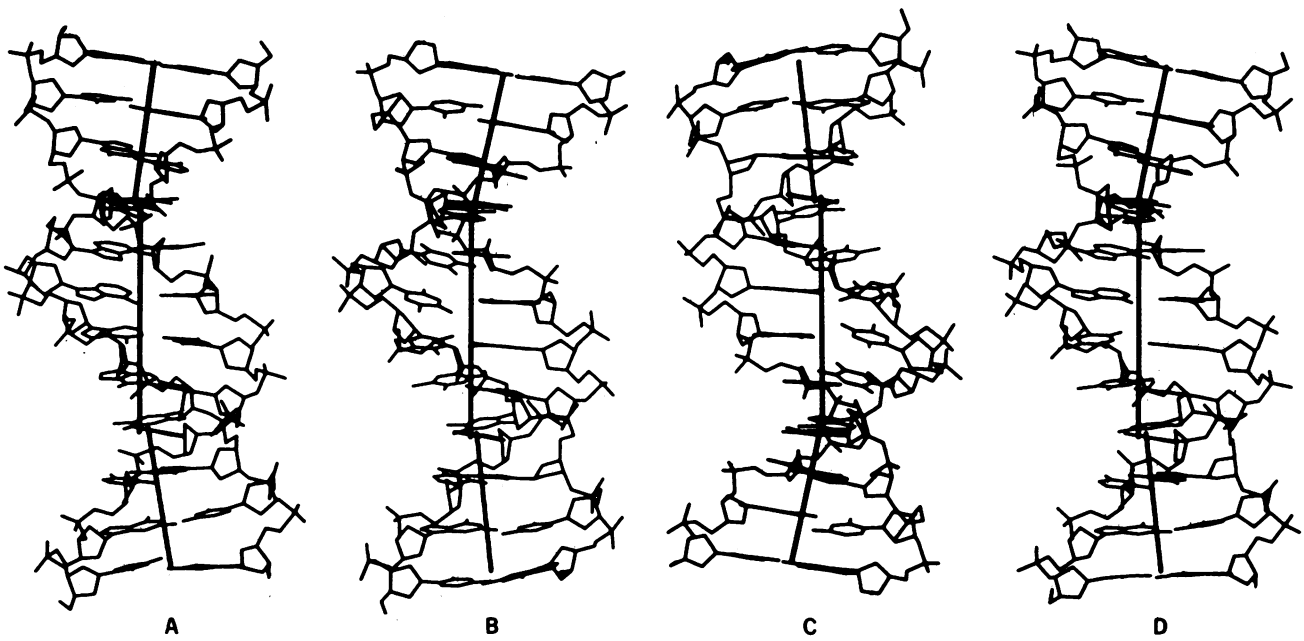


FIG. 4. Comparison of the bend found in the up and down A-tract DNAs and the Dickerson dodecamer. The helix axes of the terminal G-rich sequences and the internal $A_5$ tract are indicated by straight lines. The up and down helices (*A* and *B*) show very similar orientations of the helix axis, whereas the down helix (*C*) oriented so its sequence matches that of the up helix in *A* shows a bend in the opposite direction. For comparison, the Dickerson dodecamer (*D*) shows a very similar bend to that observed with the up and down helices.

Table 2. Bifurcated hydrogen bond lengths for four structures

| Up helix | | Down helix | | Nelson *et al.* helix (15) | | Coll *et al.* (16) | |
|---|---|---|---|---|---|---|---|
| Residues | Bifurcated H bonds, Å | Residues | Bifurcated H bonds, Å | Residues | Bifurcated H bonds, Å | Residues | Bifurcated H bonds, Å |
| $A^4 \cdot T^{20}$ | 3.7 | $A^{40} \cdot T^{32}$ | 3.3 | $A^4 \cdot T^{20}$ | 3.2 | $C^3 \cdot T^{21}$ | 3.2 |
| $A^5 \cdot T^{19}$ | 3.4 | $A^{41} \cdot T^{31}$ | 3.1 | $A^5 \cdot T^{19}$ | 3.1 | $A^4 \cdot T^{20}$ | 3.2 |
| $A^6 \cdot T^{18}$ | 3.2 | $A^{42} \cdot T^{30}$ | 2.8 | $A^6 \cdot T^{18}$ | 3.4 | $A^5 \cdot T^{19}$ | 2.7 |
| $A^7 \cdot T^{17}$ | 3.1 | $A^{43} \cdot T^{29}$ | 3.2 | $A^7 \cdot T^{17}$ | 3.2 | $A^{16} \cdot T^8$ | 3.0 |
| | | | | $A^8 \cdot T^{16}$ | 3.3 | | |
| Average | 3.4 | | 3.1 | | 3.2 | | 3.0 |

Lengths of the bifurcated hydrogen bonds in the A tract of both the up and the down helices are listed from the 5′ to the 3′ end of the A tract along with the comparable values for other A-tract structures (15, 16).

36, 37), the A-tract sequence is intrinsically bent predominantly toward the minor groove at the center of the A tract, then such a DNA molecule would not pack into this observed crystal lattice. Since the free energy stabilizing the bent conformation is small compared to the free energy of packing the DNA in a crystal lattice, the deformation of the DNA molecule that allows the most efficient packing will dominate the intrinsic A-tract bend of the DNA in solution. Thus, we conclude that the three A-tract crystal structures solved in this same crystal lattice cannot exclude the possibility that an additional A-tract structure exists in solution. Similarly, we cannot exclude the possibility that the flanking DNA bends in a direction orthogonal to that observed in these crystals.

We have concluded that the overall bend observed here in a DNA containing an A tract is a consequence of crystal lattice forces and not of the A-tract sequence. The crystal structure reported here also exhibits the additional bifurcated hydrogen bonds between the propeller twisted bases in the A+T-rich region that may serve to increase its rigidity, as observed (15, 16). As the A tract is relatively straight, the bending is localized outside this region in the crystal (15). Neither the crystal structure described here nor those previously reported (15, 16) show directly the structural basis of the DNA bending direction deduced from experiments in solution (13, 14, 36, 37). Thus, the structural basis of A-tract-induced DNA bending remains unknown.

We wish to thank D. M. Crothers for his role in the conception of this project and for valuable scientific discussions. We thank A. Klug, H. Nelson, H. Drew, and M. McCall for helpful comments. This work was supported by National Institutes of Health Grant GM-22778 (to T. A. Steitz), National Science Foundation Grant DMB-8405494, and a project grant for parisitology and tropical medicine from the MacArthur Foundation (to D. M. Crothers).

1. Marini, J. C., Levene, S. D., Crothers, D. M. & Englund, P. T. (1982) *Proc. Natl. Acad. Sci. USA* **79**, 7664–7668.
2. Hagerman, P. J. (1984) *Proc. Natl. Acad. Sci. USA* **81**, 4632–4636.
3. Griffith, J., Bleyman, M., Rauch, C. A., Kitchin, P. A. & Englund, P. T. (1986) *Cell* **46**, 717–724.
4. Wu, H. M. & Crothers, D. M. (1984) *Nature (London)* **308**, 509–513.
5. Stenzel, T. T., Patel, P. & Bastia, D. (1987) *Cell* **49**, 709–717.
6. Ryder, K., Silver, S., DeLucia, A. L., Fanning, E. & Tegtmeyer, P. (1986) *Cell* **44**, 719–725.
7. Bossi, L. & Smith, D. M. (1984) *Cell* **39**, 643–652.
8. Zahn, K. & Blattner, F. R. (1987) *Science* **236**, 416–422.
9. Snyder, M., Buchman, A. R. & Davis, R. W. (1986) *Nature (London)* **324**, 87–89.
10. Trifonov, E. N. (1980) *Nucleic Acids Res.* **8**, 4041–4053.
11. Trifonov, E. N. & Sussman, J. L. (1980) *Proc. Natl. Acad. Sci. USA* **77**, 3816–3820.
12. Ulanovsky, L. E. & Trifonov, E. N. (1987) *Nature (London)* **326**, 720–722.
13. Koo, H.-S., Wu, H.-M. & Crothers, D. M. (1986) *Nature (London)* **320**, 501–506.
14. Koo, H.-S. & Crothers, D. M. (1988) *Proc. Natl. Acad. Sci. USA* **85**, 1763–1767.
15. Nelson, H. C. M., Finch, J. T., Luisi, B. F. & Klug, A. (1987) *Nature (London)* **330**, 221–226.
16. Coll, M., Frederick, C. A., Wang, A. H.-J. & Rich, A. (1987) *Proc. Natl. Acad. Sci. USA* **84**, 8385–8389.
17. Wing, R., Drew, H., Takano, T., Broka, C., Tanaka, S., Itakura, K. & Dickerson, R. E. (1980) *Nature (London)* **287**, 755–758.
18. Rice, J. A., Crothers, D. M., Pinto, A. L. & Lippard, S. J. (1988) *Proc. Natl. Acad. Sci. USA* **85**, 4158–4161.
19. McPherson, A. (1982) *The Preparation and Analysis of Protein Crystals* (Wiley, New York).
20. Hamlin, R. (1985) *Methods Enzymol.* **114**, 416–452.
21. Anderson, D. H. (1986) Dissertation (University of California, San Diego).
22. Steigemann, W. (1974) Dissertation (Technische Universität, Munchen).
23. Holbrook, S. R. & Kim, S. H. (1984) *J. Mol. Biol.* **173**, 361–388.
24. Hendrickson, W. & Konnert, J. H. (1979) in *Biomolecular Structure, Function, Conformation and Evolution*, ed. Srinivasan, R. (Pergamon, Oxford), Vol. 1, pp. 43–57.
25. Jones, T. A. (1982) in *Computational Crystallography*, ed. Sayre, D. (Clarendon, Oxford), pp. 303–310.
26. Westhof, E., Dumas, P. & Moras, D. (1985) *J. Mol. Biol.* **184**, 119–145.
27. Sussman, J. L., Holbrook, S. R., Church, G. M. & Kim, S.-H. (1977) *Acta Crystallogr.* **33**, 800–804.
28. Fratini, A. V., Kopka, M. L., Drew, H. R. & Dickerson, R. E. (1982) *J. Biol. Chem.* **257**, 14686–14707.
29. Jurnak, F. A. & McPherson, A., eds. (1985) *Biological Macromolecules and Assemblies*, Nucleic Acids and Interactive Proteins (Wiley, New York) Vol. 2, p. 471.
30. Rhodes, D. & Klug, A. (1981) *Nature (London)* **292**, 378–380.
31. Peck, L. C. & Wang, J. C. (1981) *Nature (London)* **292**, 375–378.
32. Taylor, R., Kennard, O. & Versichel, W. (1984) *J. Am. Chem. Soc.* **106**, 244–248.
33. Dickerson, R. E., Goodsell, D. S., Kopka, M.-L. & Pjura, P. E. (1987) *J. Biomol. Struct. Dyn.* **5**, 557–579.
34. Patapoff, T. W., Thomas, G. A., Wang, Y. & Peticolas, W. L. (1988) *Biopolymers* **27**, 493–507.
35. Taillandier, E., Ridoux, J.-P., Liquier, J., Leupin, W., Denny, W. A., Wang, Y., Thomas, G. A. & Peticolas, W. L. (1987) *Biochemistry* **26**, 3361–3368.
36. Zinkel, S. & Crothers, D. M. (1987) *Nature (London)* **328**, 178–181.